

Extension of the QuickFF Force Field Protocol for an Improved Accuracy of Structural, Vibrational, Mechanical and Thermal Properties of Metal–Organic Frameworks

Louis Vanduyfhuys,* Steven Vandenbrande, Jelle Wieme, Michel Waroquier, Toon Verstraelen, and Veronique Van Speybroeck *

QuickFF was originally launched in 2015 to derive accurate force fields for isolated and complex molecular systems in a quick and easy way. Apart from the general applicability, the functionality was especially tested for metal–organic frameworks (MOFs), a class of hybrid materials consisting of organic and inorganic building blocks. Herein, we launch a new release of the QuickFF protocol which includes new major features to predict structural, vibrational, mechanical and thermal properties with greater accuracy, without compromising its robustness and transparent workflow. First, the *ab initio* data necessary for the fitting procedure may now also be derived from periodic models for the molecular system, as opposed to the earlier cluster-based models. This is essential for an accurate description of MOFs with one-dimensional metal-oxide chains. Second, cross terms that couple internal coordinates (ICs) and anharmonic contributions for bond and bend terms

are implemented. These features are essential for a proper description of vibrational and thermal properties. Third, the fitting scheme was modified to improve robustness and accuracy. The new features are tested on MIL-53(AI), MOF-5, CAU-13 and NOTT-300. As expected, periodic input data are proven to be essential for a correct description of structural, vibrational and thermodynamic properties of MIL-53(AI). Bulk moduli and thermal expansion coefficients of MOF-5 are very accurately reproduced by static and dynamic simulations using the newly derived force fields which include cross terms and anharmonic corrections. For the flexible materials CAU-13 and NOTT-300, the transition pressure is accurately predicted provided cross terms are taken into account. © 2018 Wiley Periodicals, Inc.

DOI: 10.1002/jcc.25173

Introduction

Force fields (FFs) are typically used in computational physics and chemistry to perform molecular simulations on a time and length scale that is not accessible with *ab initio* methods. On the one hand, a long simulation time is often needed to achieve sufficient convergence in the reproduction of various properties of complex systems. On the other hand, force fields are also able to access much larger length scales. The development of accurate force fields is, however, not a trivial task. This is especially true for some newer generation materials such as metal–organic frameworks (MOFs), which are hybrid materials consisting of inorganic building blocks connected by organic linkers.^[1–5] For such materials, force fields are derived with the aim to reproduce various properties such as equilibrium structure,^[6–8] vibrational density of states,^[8,9] thermal expansion,^[9–11] bulk modulus^[11,12] as well as adsorption^[13–16] and diffusion of guest molecules^[17,18] in the pores of the material. An overview of the advances that has been made in this topic is given in refs. 19,20. A specific branch of force fields which have recently been developed for applications within MOFs are the so-called coarse-grained force fields, in which atoms are united into interacting beads. They are used to perform simulations of very large systems creating perspectives to investigate the behavior of the systems on the mesoscale.^[21,22] In this paper, we do not discuss coarse grained force fields but the interested reader is referred to refs. [23–25]. Instead, this

paper describes a next generation of our QuickFF protocol which was especially designed to derive all-atom force fields from *ab initio* data in an easy and transparent way.

Due to the diversity of force fields available in the literature, it is beyond the scope of this paper to give an exhaustive review. However, to set the scene, it is important to highlight some landmark research performed in the last decades on the development of force fields for MOFs (schematically shown in Fig. 1). Many of the initial force fields used for simulations on MOFs were not specifically derived for these materials, but relied on so-called generic force fields. Examples of such generic FFs are DREIDING^[35] and UFF.^[36] UFF was extended to

L. Vanduyfhuys, S. Vandenbrande, J. Wieme, M. Waroquier, T. Verstraelen, V. Van Speybroeck

Center for Molecular Modeling (CMM), Ghent University, Technologiepark 903, 9052 Zwijnaarde, Belgium

E-mails: louis.vanduyfhuys@UGent.be, or veronique.vanspeybroeck@UGent.be

Contract grant sponsor: Fund for Scientific Research Flanders (FWO); Contract grant sponsor: Research Board of Ghent University (BOF); Contract grant sponsor: Federaal Wetenschapsbeleid (BELSPO); Contract grant number: IAP/7/05; Contract grant sponsor: H2020 European Research Council; Contract grant number: 647755 – DYNPOR (2015-2020)

This is an open access article under the terms of the Creative Commons Attribution-NonCommercial License, which permits use, distribution and reproduction in any medium, provided the original work is properly cited and is not used for commercial purposes.

© 2018 The Authors. Journal of Computational Chemistry Published by Wiley Periodicals, Inc.

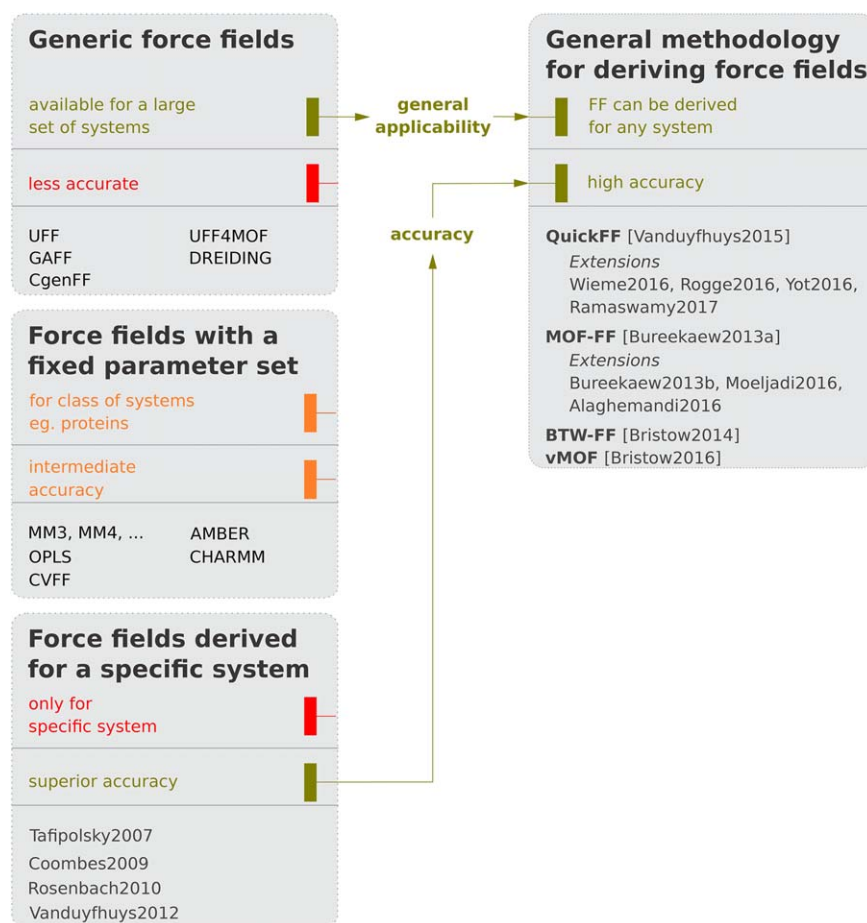


Figure 1. Graphical (non-exhaustive) representation of various classes of force fields for MOFs available in literature. On the left side, a distinction is made between three classes of force fields: generic force fields applicable to any system, force fields with a fixed parameter set and force fields derived for one specific system. On the right side, an extra class is introduced representing a general methodology for deriving accurate force fields for any system. To indicate to what degree the original methodology has been extended to systems beyond the initial application, we included a list of such extensions. The explicit references for the entries of the form NameYear in the figure are Tafipolsky2007,^[26] Coombes2009,^[27] Rosenbach2010,^[28] Vanduyfhuys2012,^[29] Vanduyfhuys2015,^[8] Wieme2016,^[10] Rogge2016,^[12] Ramaswamy2017,^[30] Bureekaew2013a,^[6] Bureekaew2013b,^[31] Moeljadi2016,^[32] Alaghemandi2016,^[33] Bristow2014,^[34] Bristow2016.^[9] [Color figure can be viewed at wileyonlinelibrary.com]

specifically simulate a broad range of MOFs^[7,37] and now covers 99% of the MOFs present in the CoRE database.^[38] Although such force fields do succeed in describing structural properties, noticeable deviations are observed for properties sensitive to vibrational modes, especially when including framework charges.^[11] As a result, more effort was invested in deriving MOF-specific force fields. Initially, such system-tailored force fields were developed as extensions of existing FFs, such as the Consistent Valence Force Fields (CVFF)^[39] applied in MIL-53(Cr),^[13] CVFF/DREIDING for MOF-5^[40] or MM3^[41] in MOF-5.^[26]

Seminal work was performed by the group of R. Schmid. In 2009, they proposed a force field for MOF-5 with parameters derived from first principles using a genetic algorithm.^[42] Since then, many other variants of system-tailored force fields appeared.^[6,29,34,43] In 2013, Schmid and coworkers extended the concept to various MOFs with the introduction of MOF-FF,^[6] which was initially applied to MOF-5, HKUST-1, DMOF-1(Zn,Cu) and UiO-66 but has been extended to other MOFs since then.^[31–33] Similarly, Bristow et al. developed vMOF (vibrational MOF) with the specific aim to describe phonon

properties of several MOFs accurately including MOF-5, UiO-66, MIL-125 and NOTT-300.^[9]

Another major point of attention in FFs is the description of non-bonding interactions. Various attempts have been made to parameterize FFs to describe adsorption of guest molecules inside the pores of MOFs. A good example is the rigid-framework FF of Kulkarni and Sholl which has been specifically constructed for simulating the adsorption of short and long alkanes in MIL-47 by fitting Lennard-Jones and Buckingham potentials to PBE-D2/vdW-D2 reference data.^[44] Vandenbrande et al. developed the Monomer Electron Density Force Field (MEDFF), a methodology to derive pairwise-additive noncovalent FFs from monomer electron densities,^[45] which was later applied to investigate methane adsorption in Zr-based MOFs.^[46]

Since a force field is in essence a parameterized mathematical expression to describe the potential energy surface of a system, with parameters chosen either according to a set of empirical rules or to reproduce experimental or *ab initio* training data, it is often not entirely clear how accurate they are. A recent assessment of several force fields on their ability to

accurately reproduce bulk moduli and thermal expansion coefficients of various MOFs, has been performed by Boyd et al.^[11] Their main conclusion was that bulk moduli are fairly well reproduced by FFs (deviation of 5% with respect to the Density Functional Theory (DFT) reference data) while the reproduction of thermal expansion coefficients is more prone to large discrepancies up to 100% from experiment. Furthermore, although generic force fields such as UFF, UFF4MOF and DREIDING without electrostatic contributions gave accurate bulk moduli, the error increased substantially with the inclusion of electrostatic contributions (up to errors of 100% depending on the partitioning scheme to obtain the atomic charges). This implies that such force fields are not adequate to simultaneously describe mechanical and adsorption properties of MOFs, because an accurate estimation of adsorption properties for polar molecules relies on an accurate representation of the electrostatic contribution, which illustrates the need for more accurate force fields for metal–organic frameworks.

In view of large screening studies, it is important to have access to a protocol for deriving force fields which can be applied in an easy and robust manner without much manual interventions. In this respect, some of the current authors introduced QuickFF^[8] in 2015, which represents an automated procedure to derive accurate FFs from first principles for isolated and complex molecular systems in a quick and easy manner. The energy expression of the force field consists of three contributions: an electrostatic part and a van der Waals part that were both assumed to be known a priori, and a covalent contribution consisting of harmonic bonds, bends and out-of-plane distances as well as dihedral terms described by a single cosine. The parameters of the covalent contributions were estimated to reproduce the *ab initio* geometry and Hessian in equilibrium. The accuracy of the resulting force fields was demonstrated for three applications. First, a set of small organic molecules was considered and for each molecule the results of the QuickFF force field were compared with the generic force fields UFF and GAFF, which illustrated the improved accuracy with respect to these universal force fields. Second, a force field was constructed for the metal–organic framework MIL-53(Al). The equilibrium geometry and unit cell of both large pore and narrow pore phases were fairly well reproduced. Third, a force field was derived for MOF-5 by applying QuickFF on the same *ab initio* input that was used for the construction of the MOF-FF force field.^[6] In this case, both unit cell parameters as well as normal mode frequencies compared well with the MOF-FF values. Since then, QuickFF has been applied on a large variety of MOFs to derive the covalent force field without any empirical input and structural, mechanical and thermal properties of these materials have been derived with relative success. As such we were able to propose a structural model for the contracted phase of MIL-53(Al)-FA,^[47] to investigate the influence of barostats on mechanical properties of MOF-5 and MIL-53(Al),^[48] the influence of the organic linker on the relative stability of large pore and narrow pore phases in MIL-47 type materials^[10] and the influence of linker defects on the mechanical stability of UiO-

66 type materials.^[12] Finally, a modified version of QuickFF has also been used to parameterize diabatic potential energy surfaces as well as the diabatic couplings for the photodissociation of thioanisole.^[49]

The applications tackled so far showed some conceptual shortcomings in the originally proposed QuickFF protocol. We applied the procedure multiple times on materials of the MIL-53 series, which are composed of one-dimensional chains. The original QuickFF protocol relied on *ab initio* data generated from small cluster models, which were cut from the periodic structure. Such a procedure is far from trivial. Second, we experienced some deficiencies in the description of vibrational and thermal properties, which led to go beyond a diagonal and harmonic energy expression. These elements lie on the basis of the development and release of a next generation of QuickFF which allows to derive force fields that reproduce structural, vibrational, thermal and mechanical properties more accurately.

The main improvements implemented in the new generation of QuickFF are the following. First of all, it is now possible to derive the necessary input data from periodic *ab initio* calculations. Second, we implemented cross terms in the energy expression, which improve the determination of structural and vibrational properties, as well as anharmonic contributions for the bonds and bends, which are essential for a better description of thermal expansion. Finally, some refinements were implemented in the fitting procedure itself to derive the force fields more accurately and efficiently. The next generation of QuickFF (i.e., QuickFF v2.2) is thoroughly tested for the computation of several structural, mechanical and thermal properties of MOFs such as MIL-53(Al), MOF-5, CAU-13 and NOTT-300. The obtained results are compared with *ab initio* and experimental data.

The remainder of the paper is structured as follows. In the “New features in QuickFF” section, we outline the details of all extensions that were implemented in QuickFF v2.2. The “Applications” section is devoted to applications of the new force fields and its improved performance is assessed. Finally, in the “Conclusions” section, the most important conclusions are given.

New Features in QuickFF

A series of extensions have been introduced in the new release to broaden the applicability and improve the accuracy of QuickFF. These extensions can be divided into three categories: (1) extensions to the input toolkit, (2) modifications of the force field energy expressions, (3) modifications in the fitting procedure. The mathematical details of these extensions will be discussed in this section, while their impact on the performance of the resulting force field is the topic of the following section.

Extension of the input toolkit for QuickFF

The input required to construct a force field with QuickFF consists of several components: the *ab initio* geometry and

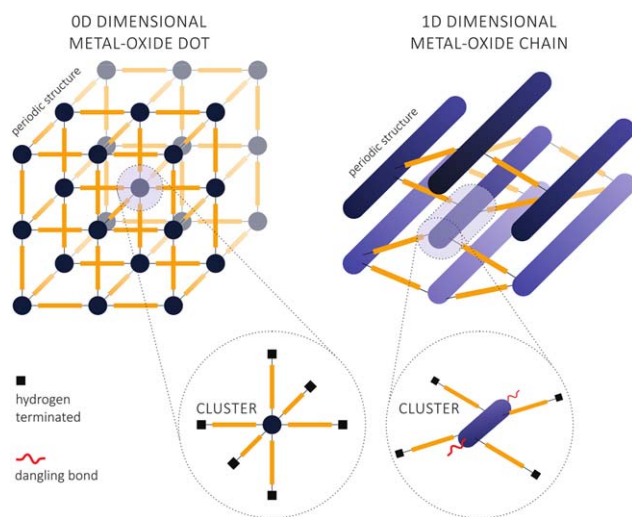


Figure 2. Schematic representation of (left) MOFs with 0D metal oxide dots and (right) MOFs with 1D metal oxide chains. The procedure to cut out cluster-based models for the generation of input data for QuickFF is also indicated. Blue spheres(tubes) represent 0D (1D) metal oxides, yellow rectangles represent organic linkers, black squares represent bonds that can easily be terminated using, for instance, hydrogen atoms, while red waves represent dangling bonds that are not trivial to terminate without influencing the electronic structure of the metal oxide. [Color figure can be viewed at wileyonlinelibrary.com]

Hessian in equilibrium of representative model systems, the electrostatic and the van der Waals interaction. In the original release of QuickFF, the model systems used for the generation of the input data consisted of clusters representative for the inorganic and organic components of the periodic system. A first extension to QuickFF, is the ability to fit the force field parameters to the *ab initio* geometry and Hessian of a periodic system instead of isolated clusters. It can be expected that the use of such periodic input data will have a major impact for MOFs such as MIL-53 and MIL-47,^[50] while it is expected to only mildly affect MOFs such as MOF-5 and UiO-66. The reason for this is the 1D-periodicity^[2] of the metal oxide chain in the MIL-53 and MIL-47 series as opposed to the 0D-dimensionality^[2] of the metal oxide dot in MOF-5 and UiO-66 as schematically shown in Figure 2. For MIL-53 type materials, we succeeded in deriving force fields with the original QuickFF version.^[10,29,47] However, it is rather artificial to cut clusters from infinitely extended chains in the material as proposing a proper termination is not a straightforward task. The boundary of the cluster leads to interactions that are not representative for the periodic system. For 1D MOFs such as MIL-53 and MIL-47 one expects a more realistic estimation of the FF parameters based on periodic input data. In MOF-5, however, the metal oxide is just a 0D-dimensional dot, for which one can easily determine a cluster in which the 0D metal oxide remains intact. Technically, the support for periodic input data was implemented by coupling QuickFF v2.2 with YAFF.^[51] YAFF is a general purpose and flexible program developed in-house to perform a variety of force field simulations. In the new release of QuickFF, every evaluation of the energy, forces or Hessian is performed by YAFF, which allows us to use periodic boundary conditions and the Ewald summation as implemented in YAFF.

An additional advantage of this coupling is the ability to use any non-bonding model implemented in YAFF. As a result, the new QuickFF release supports various non-bonding interaction models such as the dispersion model of DFT-D2,^[52] the dispersion model shared in DFT-D3^[53,54] and QMDF, the repulsion model from QMDF^[55] or the various contributions from MEDFF.^[45] The added support for these non-bonding models allows to derive covalent force fields that are complementary to many other previously derived non-bonding force fields from literature.

Modifications to the energy expression

In the previous version of QuickFF, the energy expression contained only terms diagonal in the internal coordinates, for which a simple mathematical expression was used (the entire energy expression from the original QuickFF version can be found in Section 1 of the Supporting Information). As such, harmonic potentials were used for bonds, bends and out-of-plane distances, while a single cosine was used for dihedral contributions. In the current version, this energy expression was modified to increase the accuracy of the resulting force fields with respect to the *ab initio* reference data.

(i) The first modification is the inclusion of cross terms, i.e. force field terms that explicitly couple different internal coordinates. The included cross terms are (1) angle stretch–stretch (ASS) between neighboring bonds, i.e. part of the same angle, (2) angle stretch–angle terms (ASA), (3) dihedral stretch–stretch (DSS) between the outer bonds of the same dihedral and (4) dihedral stretch–dihedral terms (DSD). The mathematical expression for these terms is given by:

$$V_{ijk}^{ASS} = K_{ijk}^{ASS} (r_{ij} - r_{0,ij}) (r_{jk} - r_{0,jk}) \quad (1)$$

$$V_{ijk}^{ASA} = \left[K_{ijk}^{ASA1} (r_{ij} - r_{0,ij}) + K_{ijk}^{ASA2} (r_{jk} - r_{0,jk}) \right] (\theta_{ijk} - \theta_{0,ijk}) \quad (2)$$

$$V_{ijkl}^{DSS} = K_{ijkl}^{DSS} (r_{ij} - r_{0,ij}) (r_{kl} - r_{0,kl}) \quad (3)$$

$$V_{ijkl}^{DSD} = \left[K_{ijkl}^{DSD1} (r_{ij} - r_{0,ij}) + K_{ijkl}^{DSD2} (r_{jk} - r_{0,jk}) + K_{ijkl}^{DSD3} (r_{kl} - r_{0,kl}) \right] \cdot \cos \left(m (\psi_{ijkl} - \psi_{0,ijkl}) \right) \quad (4)$$

The rest values in all these cross terms are taken to be identical to their diagonal counterparts, while the force constants are estimated by means of the least-squares fit of the force field Hessian to the *ab initio* Hessian (more information about the sequence of steps in the previous and current version of QuickFF can be found in Section 2.3 of the Supporting Information). In the expression for the DSD term, the factor $\cos(m(\psi - \psi_0))$ was preferred over $1 - \cos(m(\psi - \psi_0))$ as is used in MM3, because of the artificial linear force term the latter introduces on the bond as recognized by Maple et al.^[56] Cross terms that couple the neighboring bending angles in a dihedral pattern (DAA) as well as those that couple the bending angles with the dihedral angle (DAD), are implemented in QuickFF v2.2 as well. However, as initial tests revealed such terms have almost no influence, they are not discussed in this work.

(ii) A second type of modification concerns the inclusion of anharmonic contributions in the energy terms of the bond and bending motions. Such anharmonic contributions are expected to improve the description of thermal expansion because they account for the effect that it is in general easier to stretch a chemical bond than to compress it. For bond terms, two anharmonic expressions were implemented. The first is the so-called Simons–Parr–Finlan term [eq. (5)], sometimes also referred to as Fues term, which has its physical background in the simple bond charge model.^[57] The second is the MM3 bond term [eq. (6)], which corresponds to a fourth order Taylor expansion of the Morse potential.^[41] The mathematical expressions for the energy is given by:

$$V_{ij}^{\text{SPF}} = \frac{K'_{ij} r_{0,ij}^2}{2} \left(1 - \frac{r_{0,ij}}{r_{ij}} \right)^2 \quad (5)$$

$$V_{ij}^{\text{MM3}} = \frac{K''_{ij}}{2} (r_{ij} - r'_{0,ij})^2 \left[1 - \alpha (r_{ij} - r'_{0,ij}) + \frac{7}{12} \cdot \alpha^2 \cdot (r_{ij} - r'_{0,ij})^2 \right] \quad (6)$$

with $\alpha = 2.55 \text{ \AA}^{-1}$. Although the value of the force constants K'_{ij} (K''_{ij}) and rest values $r'_{0,ij}$ ($r''_{0,ij}$) can differ with respect to the harmonic bond potential, their physical interpretation remains the same. The estimation of these parameters can be done using exactly the same procedure implemented in the original QuickFF, i.e. estimation of rest values and force constants from perturbation trajectories followed by a refinement of the force constants by fitting the force field Hessian to the *ab initio* Hessian. For the bend terms, the MM3 expression^[41] was implemented, which is a sixth-order Taylor expansion in terms of the bending angle:

$$V_{ijk}^{\text{MM3}} = \frac{K'_{ijk}}{2} (\theta_{ijk} - \theta'_{0,ijk})^2 \left[1 - a_1 (\theta_{ijk} - \theta'_{0,ijk}) + a_2 \cdot (\theta_{ijk} - \theta'_{0,ijk})^2 - a_3 \cdot (\theta_{ijk} - \theta'_{0,ijk})^3 + a_4 (\theta_{ijk} - \theta'_{0,ijk})^4 \right] \quad (7)$$

with $a_1 = 0.014 \text{ deg}^{-1}$, $a_2 = 5.6 \cdot 10^{-5} \text{ deg}^{-2}$, $a_3 = 7 \cdot 10^{-7} \text{ deg}^{-3}$ and $a_4 = 2.2 \cdot 10^{-8} \text{ deg}^{-4}$. As was the case for the bonds, the force constant K'_{ijk} and rest angle $\theta'_{0,ijk}$ again have the same physical interpretation as for the harmonic term, which means that these parameters can be estimated by means of the original QuickFF procedure as well. Finally, some other minor tweaks were implemented to improve the description of several specific situations, such as bends with a rest value of 180° , bends with rest values at both 90° and 180° , dihedrals with rest values at 180° or $180^\circ/m$, and out-of-plane distances with rest values different from 0 \AA . More information about these modifications can be found in Section 2.1 of the Supporting Information.

Modifications to the fitting procedure

In the third step of the original procedure of QuickFF, the force constants are refined by fitting the force field Hessian to the *ab initio* Hessian at fixed values of the rest values. This fit was performed by means of minimizing a least-squares cost

function that measures the error between the force field Hessian and the *ab initio* reference Hessian. Two small but efficient improvements to this procedure have been implemented in QuickFF v2.2. The first is to fit the mass-weighted Hessians instead of the Hessians themselves. Hence, the least-squares cost function becomes:

$$\chi^2 = \frac{1}{2} \sum_{\alpha,\beta} \left(\left[\mathbf{M}^{-\frac{1}{2}} \mathbf{H}^{\text{ff}} \mathbf{M}^{-\frac{1}{2}} \right]_{\alpha\beta} - \left[\mathbf{M}^{-\frac{1}{2}} \mathbf{H}^{\text{ff}} (\vec{\kappa}) \mathbf{M}^{-\frac{1}{2}} \right]_{\alpha\beta} \right)^2 \quad (8)$$

in which $\vec{\kappa}$ represents the vector of force constants of the covalent terms. This concept was inspired by normal mode analysis, where the generalized eigenvalue equation of the Hessian, which also contains the mass matrix, is transformed to a regular eigenvalue of the mass-weighted Hessian. The eigenvalues of the mass-weighted Hessian then directly correspond to the (square of the) frequencies. Hence, it can be anticipated that fitting the mass-weighted Hessian will result in a better reproduction of the frequencies, which is highly desirable to accurately describe the thermodynamic properties of the system, such as the free energy, expressed in terms of these frequencies.

The second improvement is related to the numerical stability of the solution. In the original version of QuickFF, the number of degrees of freedom, i.e. the number of force constants, was limited due to the absence of cross terms. This in turn resulted in a set of equations with a numerically stable solution. However, due to addition of cross terms, the number of degrees of freedom significantly increases, especially in the case of adding cross terms for both angle and dihedrals patterns. This was found to increase the redundancy in the set of equations resulting in numerically less stable solutions. This redundancy was removed by means of a singular value decomposition (SVD) and the least-square cost function was minimized approximately in a non-redundant subspace of the space of force constants. As a result of this procedure, lower and upper bounds could no longer be taken into account. Because such bounds are used to avoid negative force constants for bonds, bends and out-of-plane distances as well as to avoid unphysically large dihedral force constants, this SVD was only used to fit the cross terms separately. The mathematical details of this procedure can be found in Section 2.2 of the Supporting Information. Finally, due to the introduction of cross terms and the added feature of the SVD, some modifications were also required in the sequence of the various steps of QuickFF v2.2. This sequence, as well as the differences with the original QuickFF, is given and discussed in Section 2.3 of the Supporting Information.

Applications

All extensions implemented in QuickFF v2.2 were proposed with the aim of improving the description of structural, vibrational, thermal and mechanical properties of MOFs. However, an initial test was performed on a set of small organic molecules, similar as was done in the original QuickFF version.^[8] This allows to test the new force fields and to illustrate the

Table 1. Values for the IDs of the force fields used in this work.

Force field ID	Mass-weighting	Cross terms		(An)harmonicity			
		Angles	Dihedrals	Harm	Fues	MM3	Harm→MM3 ^[a]
MDH	✓	✗	✗	✓			
MCAH	✓	✓	✗	✓			
MCADH	✓	✓	✓	✓			
MCAF	✓	✓	✗		✓		
MCAM	✓	✓	✗			✓	
MCAH-M	✓	✓	✗				✓

[a] Harmonic contributions for the bonds and bends were fitted with QuickFF v2.2, however, these terms were replaced with MM3 anharmonic terms afterwards without changing the parameters.

improved reproduction of the *ab initio* frequencies, which is necessary for a good reproduction of various thermodynamic properties such as the free energy. Further details on this validation can be found in Section 3 of the Supporting Information. The main conclusion is that the presence of cross terms and the use of a mass-weighted Hessian in the fitting procedure decrease the error in reproducing the *ab initio* normal mode frequencies by 60%.

In this section, we investigate the impact of the various extensions on the description of structural, thermal and mechanical properties of several MOFs. First, we demonstrate that the use of periodic *ab initio* input, the inclusion of cross terms and the inclusion of anharmonic bonds and/or bends has a positive influence on the reproduction of the geometry, normal mode frequencies and temperature dependence of the free energy in the normal mode approximation of the metal organic framework MIL-53(Al). Second, we investigate the role of anharmonicity of the bond and bend terms on the bulk modulus and thermal expansion of MOF-5 and compare with *ab initio* and experimental data from literature. Finally, we investigate the pressure-induced transitions of CAU-13 and NOTT-300 at 0 K and compare with *ab initio* results from literature.

The extensions implemented in the new release are multi-fold. To assess the importance of each modification individually, we tested various options and introduced a transparent notation, which assists the reader in the discussion. Force fields will be denoted as FF_{ID}^M. The first label M indicates the molecular model used for the *ab initio* input: this can represent a cluster model (M = C) or a periodic model (M = P). The label ID identifies the considered modifications of the force field. An overview of the different variants applied in this work is given in Table 1.

Geometry, frequency spectrum and free energy of MIL-53(Al)

The investigation of the small organic molecules showed that cross terms improve the description of the normal mode frequencies. However, it remains to be validated to what extent this is also true for metal–organic frameworks. To this end, we consider the flexible metal–organic framework MIL-53(Al), which was also studied earlier by the presenting authors using the original QuickFF. MIL-53(Al) consists of one-dimensional aluminum-oxide chains connected by 1,4-benzenedicarboxylate linkers. In earlier force field developments,^[8,29] clusters

were cut out from the periodic system to generate the necessary *ab initio* input. With the new release of QuickFF, we now have the ability to extract the required input from periodic DFT data and to discuss the difference in performance of the two force fields resulting from the clusters and the periodic model (see Fig. 3). The cluster was cut out of the periodic system centered around a diamond-shaped channel in which the Al(OH) chains are terminated using water molecules and hydroxyl groups. Notice that these clusters are different from those used in our earlier force field.^[29] In the latter, two

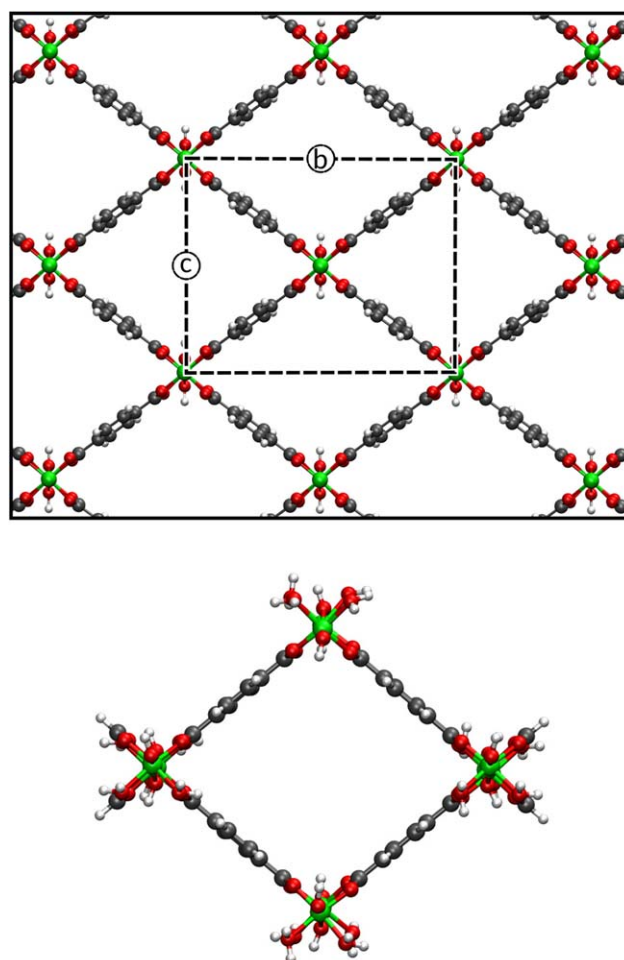


Figure 3. Illustration of (top) the periodic structure of MIL-53(Al) and (bottom) the isolated cluster cut out of the periodic structure. [Color figure can be viewed at wileyonlinelibrary.com]

Table 2. Internal coordinates (ICs), unit cell and normal mode frequencies of MIL-53(Al) in equilibrium as predicted by various force fields, compared with the *ab initio* reference data.

	AI	FF _{MDH} ^P	FF _{MCAH} ^P	FF _{MCAHDH} ^P	FF _{MCAH} ^C	FF _{MCAH} ^P	FF _{MCAH-M} ^P
RMSD of ICs							
Bonds [Å]	Ref.	0.008	0.004	0.005	0.026	0.005	0.004
Bends [deg]	Ref.	1.1	1.1	1.1	7.7	1.2	1.0
Dihedrals [deg]	Ref.	6.9	6.9	6.9	9.4	6.9	6.9
Cell lengths [Å]							
<i>a</i>	6.675	6.723	6.666	6.667	6.925 ^[a]	6.652	6.675
<i>B</i>	17.164	16.576	16.722	16.698	18.813 ^[a]	16.748	16.654
<i>c</i>	12.460	13.480	13.227	13.263	5.700 ^[a]	13.194	13.317
Cell angles [deg]							
α	90.0	90.0	90.0	90.0	92.5 ^[a]	90.0	90.0
β	90.0	90.0	90.0	90.0	87.7 ^[a]	90.0	90.0
γ	89.2	90.0	89.8	89.8	89.9 ^[a]	90.2	90.1
Cell volume [Å³]							
	1427	1508	1474	1476	741 ^[a]	1470	1481
Frequency error [cm⁻¹]^[b]							
RMSD	Ref.	35.35	24.31	20.93	37.13	21.95	44.06 (20.88) ^[c]
MD	Ref.	-19.31	7.61	5.08	24.14	4.70	10.22 (5.14) ^[c]
RVD	Ref.	29.60	23.09	20.31	28.22	21.44	42.85 (20.24) ^[c]

[a] According to FF_{MCAH}^C the large pore phase is not a stable configuration at 0 K. As a result, a geometry optimization results in the closed pore phase. [b] Three measures of errors between force field and *ab initio* frequencies are used: (RMSD) the root-mean-square deviation as a measure for the total error, (MD) the mean deviation as a measure for the systematic error and (RVD) the root of the variation of the deviation as measure for the non-systematic error. These three measures obey the relation $\text{RMSD}^2 = \text{MD}^2 + \text{RVD}^2$. [c] The frequencies of the O—H stretch along the inorganic chain are overestimated by 300 cm⁻¹, which is the reason for the large errors on the frequencies. The numbers between parenthesis give the error on the frequencies in which these O—H stretches are excluded.

clusters were considered, one for the inorganic part and one for the organic part. Here, we opt for a single cluster centered around the diamond pore to more realistically mimic the geometric constraints in the periodic structure. The periodic model consists of a single conventional unit cell of the material in its large pore phase. The geometry and Hessian in equilibrium for the cluster and the periodic model are computed with Gaussian 09^[58] and the Vienna Ab Initio Simulation Package (VASP)^[59,60] respectively, both using DFT with the PBE functional.^[61] More details on these *ab initio* computations can be found in Section 4.1 of the Supporting Information. Note that for a 1D material such as MIL-53(Al), it is more natural to use periodic input data. For 0D materials, small clusters may be equally suited and are also computationally more attractive since generating periodic Hessians to an acceptable level of accuracy is a computational rather intensive task.

Various force fields were derived and applied to optimize the structure of MIL-53(Al), to compute the Hessian in equilibrium and to extract the normal mode frequencies. Table 2 illustrates the ability of these force fields to reproduce the *ab initio* internal coordinates (ICs), unit cell parameters and normal mode frequencies. As anticipated, the force field based on periodic input (FF_{MCAH}^P) clearly outperforms the force field based on cluster data (FF_{MCAH}^C). Surprisingly, according to FF_{MCAH}^C the material collapses to the closed pore structure when performing a geometry optimization starting from the large pore phase. Hence, according to the force field FF_{MCAH}^C the large pore phase is not an equilibrium state at 0 K which contradicts the periodic *ab initio* input. Next, we investigate the influence of cross terms on the performance of the force fields derived from periodic input. Although FF_{MCAH}^P and FF_{MCAHDH}^P reproduce the geometry and unit cell slightly better than FF_{MDH}^P we can conclude that the influence of cross terms

on the equilibrium geometry is limited. However, cross terms do have a significant impact on the reproduction of normal mode frequencies, as the total error (RMSD) decreases from 35 cm⁻¹ for FF_{MDH}^P to 24 cm⁻¹ for FF_{MCAH}^P and 21 cm⁻¹ for FF_{MCAHDH}^P which is primarily due to a decrease in the systematic error (MD). Furthermore, by investigating the frequencies in more detail, we observe that the frequencies are reproduced much better mainly in the range of 100–1000 cm⁻¹ (see Section 4.3 of the Supporting Information). Finally, the force field FF_{MCAH}^P performs very similar as FF_{MCAH}^C indicating that anharmonic terms are only of minor importance for the reproduction of geometry and normal mode frequencies. The force field FF_{MCAH-M}^P performs very similar as FF_{MCAH}^P as well, except for reproducing the frequencies for which it does not seem to perform very well at first sight. However, the large error is primarily due to a deviation in the frequencies of the O—H stretches. This can be seen by considering the errors on the frequencies excluding these O—H stretches, which are given by the numbers between parenthesis in Table 2. The underlying reason for the larger errors on the OH frequencies when introducing the anharmonic corrections *a posteriori* (i.e., modifying FF_{MCAH}^P to FF_{MCAH-M}^P), can be found in the large contribution of the electrostatic interactions for that bond. When changing the harmonic term to the anharmonic MM3 term without refitting the parameters, the balance between covalent and electrostatic contributions will change, which results in a different curvature of the total energy along the O—H bond. However, the impact of this difference on the computation of properties such as geometry, bulk modulus, thermal expansion and transition pressures is very small because the O—H bond does not play a crucial role in the processes governing those properties. Overall, the assessment on a 1D-dimensional MOF shows that using periodic input and adding

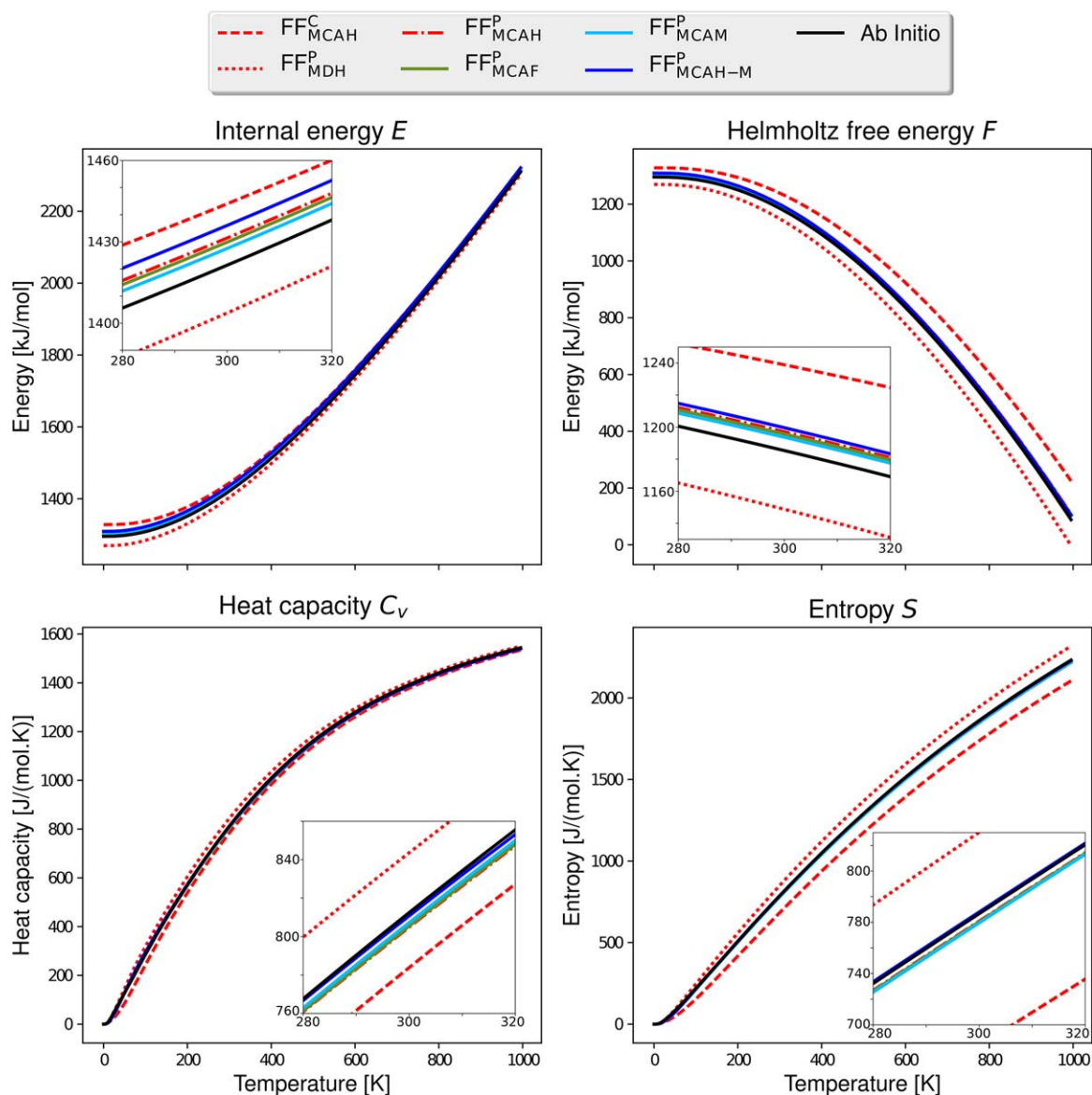


Figure 4. Internal energy E , Helmholtz free energy F , heat capacity C_v and entropy S of the periodic MIL-53(AI) in the large pore phase as function of temperature in the harmonic oscillator approximation according to the *ab initio* reference as well as several force fields as outlined in the main text. [Color figure can be viewed at wileyonlinelibrary.com]

cross terms results in a crucial improvement of the description of the normal mode frequencies.

To further illustrate the impact of improving the description of the frequencies, we computed the internal energy E , Helmholtz free energy F , entropy $S = -(\partial F / \partial T)_{N,V}$ and heat capacity $C_v = (\partial E / \partial T)_{N,V}$ of MIL-53(AI) with a fixed unit cell given by the optimized large pore phase, as a function of temperature T in the quantum-harmonic approximation using the computed normal mode frequencies:

$$E(T) = \sum_{i=1}^{N_{\omega}} \left(\frac{\hbar\omega_i}{2} + \frac{\hbar\omega_i}{\exp(\beta\hbar\omega_i) - 1} \right) \quad (9)$$

$$F(T) = \sum_{i=1}^{N_{\omega}} \left(\frac{\hbar\omega_i}{2} + k_B T \ln [1 - \exp(-\beta\hbar\omega_i)] \right) \quad (10)$$

$$C_v(T) = k_B \sum_{i=1}^{N_{\omega}} \left(\frac{\hbar\omega_i}{k_B T} \right)^2 \frac{\exp(\beta\hbar\omega_i)}{(\exp(\beta\hbar\omega_i) - 1)^2} \quad (11)$$

$$S(T) = k_B \sum_{i=1}^{N_{\omega}} \left(\frac{\beta\hbar\omega_i}{\exp(\beta\hbar\omega_i) - 1} - \ln [1 - \exp(-\beta\hbar\omega_i)] \right) \quad (12)$$

These observables were computed using both the *ab initio* frequencies, as well as the frequencies according to various force fields. The results are plotted in Figure 4, from which it is clear that the force field without cross terms (FF_{MDH}^P) underestimates the internal energy and the free energy, while the force field derived from a cluster (FF_{MCAH}^C) overestimates both energies. This can be traced back to a large negative respectively positive systematic error on the frequencies given by the MD in Table 2. All other force fields, i.e. force fields derived from periodic input that include cross terms, either with or without

anharmonic bond and/or bend contributions, reproduce the given thermodynamic properties very well, with FF_{MCAH-M}^P performing the best. Hence, we can conclude that using periodic *ab initio* input data and incorporating cross terms are essential to reproduce the temperature-dependent vibrational free energy of MIL-53(Al), while the presence of anharmonicities in this particular case is of secondary importance.

Thermal and mechanical properties of MOF-5

As a second application we investigate the role of anharmonic terms in the calculation of the bulk modulus and volumetric thermal expansion coefficient of MOF-5. MOF-5 is a metal-organic framework consisting of Zn_4O bricks connected by 1,4-benzenedicarboxylate (BDC) linkers. The resulting periodic structure contains zero-dimensional Zn_4O metal-oxides,^[2] in contrast to MIL-53(Al) which contains one-dimensional Al(OH) chains. As a result, one can easily cut a representative cluster from the periodic structure without distorting the local electronic structure too much. It is a clear example that one needs to make a clearly motivated choice for the selection of the input data. In this case, to construct a force field for MOF-5, a cluster was cut out of the periodic system centered around a Zn_4O metal oxide brick, terminated with 6 benzene carboxylate molecules (see Fig. 5). The geometry and Hessian of the cluster in equilibrium were computed with Gaussian 09^[58] using DFT with the B3LYP functional^[62-66] and the 6-311++G(d,p) basis set.^[67-69] This *ab initio* data was also used previously as input for MOF-FF^[6] as well as for QuickFF v1.^[8]

Four different force fields are considered, FF_{MCAH}^C containing only harmonic contributions, and FF_{MCAH}^C , FF_{MCAH}^M and FF_{MCAH-M}^C representing various models for anharmonic bonds and bends (see Table 1 for the FF nomenclature). Similar as for MIL-53(Al), we observe that all force fields containing cross terms reproduce the thermal corrections to the various thermodynamic properties appropriately. Further inclusion of anharmonic contributions only has a minimal effect on the results (see Section 5.2 of the Supporting Information for more details). The bulk moduli were computed by means of an equation-of-state fit to the results of geometry optimizations at various fixed pressures, while the thermal expansion coefficients were computed by means of a fit to the results of molecular dynamics simulations in the *NPT* ensemble at various temperatures. More details can be found in Section 5.3 of the Supporting Information. By comparing the results for the various force fields in Table 3, we see that the anharmonic terms have little effect on the bulk modulus, however, they improve the description of the thermal expansion coefficient. Using the anharmonic energy contributions for bonds and bends from the MM3 force field results in a thermal expansion coefficient that is very close to the experimental value. Furthermore, FF_{MCAH-M}^C predicts a volumetric thermal expansion coefficient of $-4.2 \cdot 10^{-5} \text{ K}^{-1}$, which lies exactly in the experimental range, while the bulk modulus is only slightly underestimated compared to DFT.

It is important to note that an accurate reproduction of the thermal expansion coefficient using a force field is far from

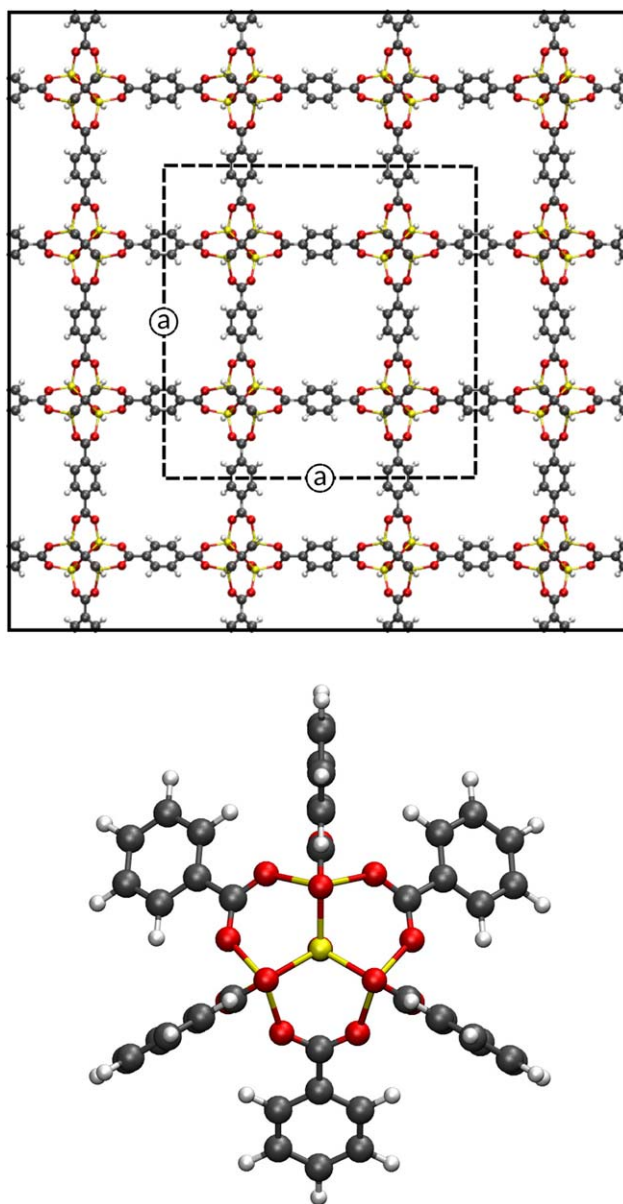


Figure 5. Illustration of (top) the periodic structure of MOF-5 and (bottom) the isolated cluster cut out of the periodic structure. [Color figure can be viewed at wileyonlinelibrary.com]

trivial, as illustrated by the wide range of values predicted by different force fields,^[11] ranging from $-1.6 \cdot 10^{-5} \text{ K}^{-1}$ for BTW-FF^[34] to $-7.9 \cdot 10^{-5} \text{ K}^{-1}$ for UFF4MOF^[7] as reported in Table 3. Furthermore, it was also shown that force fields such as UFF, UFF4MOF and DREIDING, including electrostatic contributions give rise to even larger fluctuations on both bulk moduli and thermal expansion coefficients.^[11] The force fields derived in this work are much less prone to such fluctuations, because the electrostatic contribution is computed using Gaussian smeared charges, effectively damping strong interactions of alternating sign between atoms in highly polarized and dense systems such as the inorganic bricks in metal-organic frameworks. Taking all these elements into account, we can conclude that the MCAH-M force field (with anharmonic MM3 bonds and bends) succeeds very well in reproducing the DFT

Table 3. Comparison of the bulk modulus (B) at 0 K and volumetric thermal expansion coefficient (α) in the range of 100–300 K of MOF-5 as predicted by four force fields with periodic DFT and/or experimental values.

	B [GPa]	α [10^{-5} K^{-1}]
Exp. ^[a]	–	–3.6 to –4.8
DFT ^[b]	16.3–18.5	–
<i>Force fields from literature^[c]</i>		
BTW-FF	12.0, 13.6	–1.6, –0.9
UFF4MOF	16.8	–7.9
DWES	17.5	–5.7
<i>QuickFF v2.2</i>		
FF _{MCAH} ^C	17.1	–6.5
FF _{MCAF} ^C	17.2	–5.9
FF _{MCAM} ^C	17.5	–5.0
FF _{MCAH-M} ^C	15.1	–4.2

[a] Experimental values taken from refs. [70–72]. [b] DFT values (both LDA and GGA) taken from ref. [73] and references therein. [c] BTW-FF values taken from refs. [11,34], DWES^[40] and UFF4MOF^[7] values are taken from ref. [11].

value of the bulk modulus and the experimental negative thermal expansion coefficient.

Pressure-induced transitions of CAU-13 and NOTT-300

As a final application, we construct force fields for NOTT-300^[74] and CAU-13^[75] (see Fig. 6) with the new generation of QuickFF and investigate their behavior when exposed to external mechanical pressure at 0 K. Both materials belong to the class of flexible MOFs, and to the best of our knowledge, no force field has been developed for CAU-13, while for NOTT-300 only one force field is available in the literature.^[9] NOTT-300 consists of Al atoms connected to each other by means of *cis*- μ_2 -OH groups giving rise to helix-like Al(OH) chains, which are in turn connected to each other through biphenyl-3,3',5,5'-tetracarboxylate linkers. CAU-13 is similar to MIL-53(Al), but the 1,4-benzenedicarboxylate linkers are replaced by *trans*-1,4-cyclohexanedicarboxylate linkers. The mechanical behavior of these two materials has already been investigated by Ortiz et al.^[76] by means of periodic DFT simulations. For both materials they observed a structural transition. Here, we investigate the behavior for both materials using the MDH, MCAH, MCAH-M and MCAM variants of force fields derived from periodic DFT input. For both materials, a pressure scan is performed in which the structure is equilibrated under external mechanical pressure for a given range of pressures (Fig. 7). Furthermore, the pressure scan is performed both in a forward manner, increasing the pressure starting from its lowest value (solid lines in Fig. 7), as well as in a backward manner, i.e. decreasing the pressure starting from its highest value (dashed lines in Fig. 7). In this way, possible hysteresis phenomena can be detected. More details about the *ab initio* input data as well as the simulation details can be found in Section 6 of the Supporting Information.

Figure 7 shows the result of the pressure scan performed for CAU-13 and NOTT-300. In the case of CAU-13 (top pane), one can clearly observe that all four force fields give very similar results for pressures of 0 MPa and higher, while for

negative pressures a clear difference is noticed between FF_{MDH}^P on the one hand and the other force fields on the other hand. This was to be expected, since each force field was fitted to reproduce the same *ab initio* equilibrium geometry, and at 0 MPa each force field will predict this equilibrium structure. Furthermore, as it was shown in previous sections, cross terms are essential for an accurate representation of the potential energy surface, hence, it is also not surprising that FF_{MDH}^P gives deviating results. All force fields reveal a transition at a pressure between –300 MPa and –200 MPa, similar to the transition found by Ortiz et al. at around –500 MPa. However, they observed hysteresis in the transition, which is not the case for the force field simulations presented here do not. Similar results are found for NOTT-300 (bottom pane of Fig. 7). On the one hand, all four force fields give very similar results for the large pore branch, i.e. the structures with a volume larger than 2500 Å³. This can again be attributed to the fact that these structures are similar to the *ab initio* structure to which the force fields were fitted. Furthermore, all force fields predict a

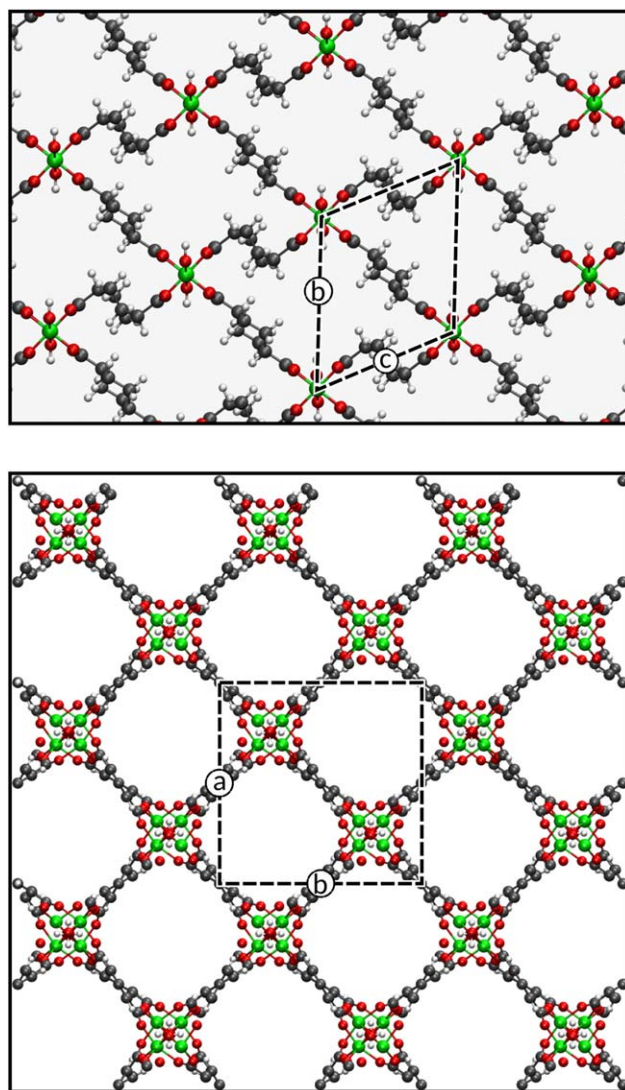


Figure 6. Structure of the metal–organic frameworks CAU-13 (top) and NOTT-300 (bottom). [Color figure can be viewed at wileyonlinelibrary.com]

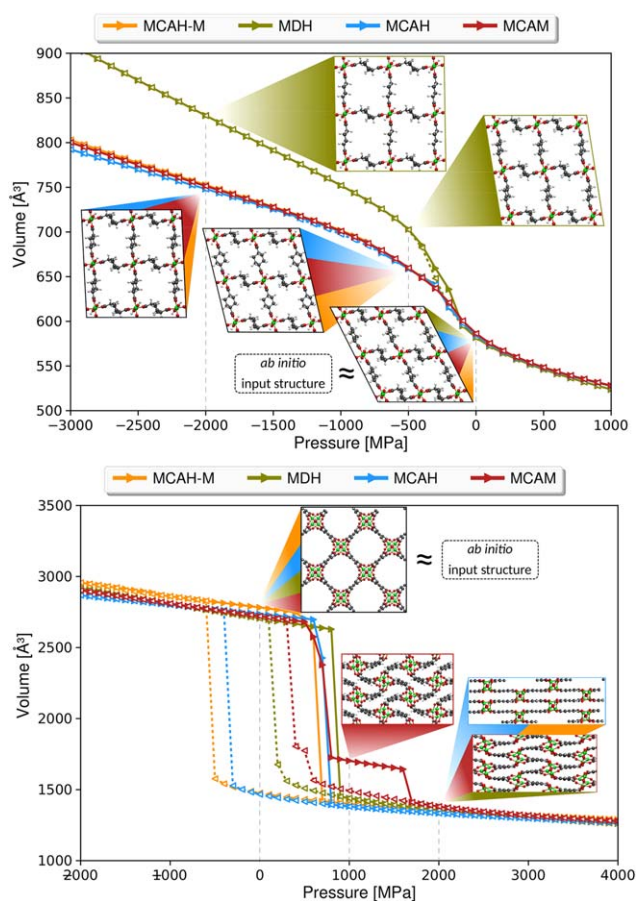


Figure 7. Volume versus pressure profile for (top) CAU-13 and (bottom) NOTT-300 using various force fields. Solid lines indicate the forward branch (increasing pressure), while dashed lines indicate the backward branch (decreasing pressures). Inset figures indicate the structure at a certain pressure. The force field that corresponds with each structure is indicated with the color according to the legend. As indicated on the figure, the structure at 0 MPa according to each force field corresponds very well with the *ab initio* input data each force field was fitted to. Higher resolution versions of these figures are included in Section 6.3 of the Supporting Information. [Color figure can be viewed at wileyonlinelibrary.com]

transition toward a smaller volume phase at a pressure between 600 and 900 MPa, which is in very good agreement with the results of Ortiz et al., who found a transition at around 700 MPa at 300 K by means of *ab initio* (PBE-D2) molecular dynamics simulations in the *NPT* ensemble. On the other hand, the force fields predict different structures after the transition. The FF_{MCAH}^P and FF_{MCAH-M}^P force fields result in a very symmetric closed pore phase as indicated in the figure (blue/orange structure at 2000 MPa in the bottom pane of Fig. 7), while the FF_{MDH}^P and FF_{MCAM}^P force fields result in closed pore phases with more distorted channels (red/green structure at 2000 MPa). Furthermore, instead of going directly from the large pore to the closed pore phase, FF_{MCAM}^P predicts an intermediate phase which exhibits similarly distorted channels (red structure at 1000 MPa). Finally, it is known that even at the *ab initio* level of theory, dispersion has a large influence on the $E(V)$ profile at 0 K.^[77,78] Therefore, we also tested the influence of the van der Waals model by comparing van der Waals terms from the MM3 force field with those of the UFF force field (see

Section 6.4 of the Supporting Information). A large impact on the resulting pressure profiles was observed, as both the large pore and closed pore volumes showed a significant differences between the van der Waals models. The transition pressures for CAU-13 (closed pore to large pore phase) and NOTT-300 (large pore to closed pore phase) are, however, less affected by the different van der Waals model. The results for NOTT-300 discussed here could indicate that various plausible closed pore structures exist for NOTT-300, separated by small energy barriers. Depending on the initial structure as well as the exact balance between the various contributions to the force field, one structure will be preferred over the other. However, it could be anticipated that the pressure profile becomes less prone to this balance at elevated temperature, since smaller energy barriers are easier to overcome at higher temperature. Such an investigation is, however, beyond the scope of this work.

Conclusions

Within this paper, we introduced a new release of QuickFF (QuickFF v2.2) to derive reliable force fields for metal–organic frameworks in a transparent and easy way. The new release essentially covers modifications in three different aspects. A first modification allows us to use periodic *ab initio* input to derive force fields from, avoiding the need to disturb the chemical environment when cutting clusters from periodic structures. The second modification involves extensions of the energy expression such as anharmonic bond and bends contributions as well as cross terms. The third modification concerns the fitting procedure and applies mass-weighting to the Hessian cost function for the estimation of force constants.

To illustrate how these modifications increase the accuracy of the resulting force fields, we considered four different metal–organic frameworks. First, it was shown for MIL-53(Al) that deriving the force field from periodic *ab initio* input data as well as adding cross terms is essential to accurately describe the normal mode frequencies. Second, force fields that include anharmonic bond and bend contributions are able to accurately reproduce both bulk modulus and the negative thermal expansion of MOF-5, resulting in a very good agreement with DFT calculations or experimental measurements. Finally, the volume versus pressure profiles were computed for NOTT-300 and CAU-13 at 0 K and compared with *ab initio* simulations from literature. Although in the case of NOTT-300, different force fields predict different closed pore phases, both materials were shown to exhibit transitions at pressures comparable to the *ab initio* values from literature. In conclusion, QuickFF has been updated with multiple modifications that result in force fields with increased accuracy able to describe structural, vibrational, mechanical and thermal properties of various metal–organic frameworks.

Program Availability

The Python code of QuickFF v2.2.0 including all modifications discussed in this work can be downloaded from the web-


interface to the revision control system Git: <http://github.com/molmod/QuickFF>.

Acknowledgments

The computational resources (Stevin Supercomputer Infrastructure) and services used in this work were provided by the VSC (Flemish Supercomputer Center), funded by Ghent University, FWO and the Flemish Government – department EWI.

Keywords: QuickFF v2.2 · automated software · force field development · metal–organic frameworks · molecular simulation

How to cite this article: L. Vanduyfhuys, S. Vandenbrande, J. Wieme, M. Waroquier, T. Verstraelen, V. Van Speybroeck. *J. Comput. Chem.* **2018**, *39*, 999–1011. DOI: 10.1002/jcc.25173

 Additional Supporting Information may be found in the online version of this article.

- [1] S. Kitagawa, S. I. Noro, R. Kitaura, *Angew. Chem. Int. Ed.* **2004**, *43*, 2334.
- [2] G. Férey, *Chem. Soc. Rev.* **2008**, *37*, 191.
- [3] H. Furukawa, K. E. Cordova, M. O’Keeffe, O. M. Yaghi, *Science* **2013**, *341*, 1230444.
- [4] A. Schneemann, V. Bon, I. Schwedler, I. Senkovska, S. Kaskel, R. A. Fischer, *Chem. Soc. Rev.* **2014**, *43*, 6062.
- [5] G. Maurin, C. Serre, A. Cooper, G. Férey, *Chem. Soc. Rev.* **2017**, *46*, 3104.
- [6] S. Bureekaew, S. Amirjalayer, M. Tafipolsky, C. Spickermann, T. K. Roy, R. Schmid, *Phys. Status Solidi B* **2013**, *250*, 1128.
- [7] M. A. Addicoat, N. Vankova, I. F. Akter, T. Heine, *J. Chem. Theory Comput.* **2014**, *10*, 880.
- [8] L. Vanduyfhuys, S. Vandenbrande, T. Verstraelen, R. Schmid, M. Waroquier, V. Van Speybroeck, *J. Comput. Chem.* **2015**, *36*, 1015.
- [9] J. K. Bristow, J. M. Skelton, K. L. Svane, A. Walsh, J. D. Gale, *Phys. Chem. Chem. Phys.* **2016**, *18*, 29316.
- [10] J. Wieme, L. Vanduyfhuys, S. M. J. Rogge, M. Waroquier, V. Van Speybroeck, *J. Phys. Chem. C* **2016**, *120*, 14934.
- [11] P. G. Boyd, S. M. Moosavi, M. Witman, B. Smit, *J. Phys. Chem. Lett.* **2017**, *8*, 357.
- [12] S. M. J. Rogge, J. Wieme, L. Vanduyfhuys, S. Vandenbrande, G. Maurin, T. Verstraelen, M. Waroquier, V. Van Speybroeck, *Chem. Mater.* **2016**, *28*, 5721.
- [13] F. Salles, A. Ghoufi, G. Maurin, R. G. Bell, C. Mellot-Draznieks, G. Férey, *Angew. Chem. Int. Ed.* **2008**, *47*, 8487.
- [14] A. Ghysels, L. Vanduyfhuys, M. Vandichel, M. Waroquier, V. Van Speybroeck, B. Smit, *J. Phys. Chem. C* **2013**, *117*, 11540.
- [15] L. Vanduyfhuys, A. Ghysels, S. Rogge, R. Demuyck, V. Van Speybroeck, *Mol. Simul.* **2015**, *41*, 1311.
- [16] M. Witman, S. Ling, S. Jawahery, P. G. Boyd, M. Haranczyk, B. Slater, B. Smit, *J. Am. Chem. Soc.* **2017**, *139*, 5547.
- [17] F. Salles, H. Jobic, T. Devic, V. Guillerm, C. Serre, M. M. Koza, G. Férey, G. Maurin, *J. Phys. Chem. C* **2013**, *117*, 11275.
- [18] S. Amirjalayer, M. Tafipolsky, R. Schmid, *Angew. Chem. Int. Ed.* **2007**, *46*, 463.
- [19] G. Fraux, F. X. Coudert, *Chem. Commun.* **2017**, *53*, 7211.
- [20] P. G. Boyd, Y. Lee, B. Smit, *Nat. Rev. Mater.* **2017**, *2*, 17037.
- [21] J. P. Durholt, R. Galvelis, R. Schmid, *Dalton Trans.* **2016**, *45*, 4370.
- [22] R. Semino, J. P. Durholt, R. Schmid, G. Maurin, *J. Phys. Chem. C* **2017**, *121*, 21491.
- [23] G. Voth, *Coarse-Graining of Condensed Phase and Biomolecular Systems*; CRC Press/Taylor and Francis Group, Boca Raton, Florida, **2009**.
- [24] R. Potestio, C. Peter, K. Kremer, *Entropy* **2014**, *16*, 4199.
- [25] A. Karimi-Varzaneh, F. Müller-Plathe, *Top. Curr. Chem.* **2011**, *307*, 295.
- [26] M. Tafipolsky, S. Amirjalayer, R. Schmid, *J. Comput. Chem.* **2007**, *28*, 1169.
- [27] D. S. Coombes, F. Cora, C. Mellot-Draznieks, R. G. Bell, *J. Phys. Chem. C* **2009**, *113*, 544.
- [28] N. Rosenbach, Jr., A. Ghoufi, I. Deroche, P. L. Llewellyn, T. Devic, S. Bourrelly, C. Serre, G. Férey, G. Maurin, *Phys. Chem. Chem. Phys.* **2010**, *12*, 6428.
- [29] L. Vanduyfhuys, T. Verstraelen, M. Vandichel, M. Waroquier, V. Van Speybroeck, *J. Chem. Theory Comput.* **2012**, *8*, 3217.
- [30] P. Ramaswamy, J. Wieme, E. Alvarez, L. Vanduyfhuys, J. P. Itie, P. Fabry, V. Van Speybroeck, C. Serre, P. G. Yot, G. Maurin, *J. Mater. Chem. A* **2017**, *5*, 11047.
- [31] S. Bureekaew, R. Schmid, *CrystEngComm* **2013**, *15*, 1551.
- [32] A. M. P. Moeljadi, R. Schmid, H. Hirao, *Can. J. Chem.* **2016**, *94*, 1144.
- [33] M. Alaghemandi, R. Schmid, *J. Phys. Chem. C* **2016**, *120*, 6835.
- [34] J. K. Bristow, D. Tiana, A. Walsh, *J. Chem. Theory Comput.* **2014**, *10*, 4644.
- [35] S. Mayo, B. Olafson, W. Goddard, *J. Phys. Chem.* **1990**, *94*, 8897.
- [36] A. K. Rappé, C. J. Casewit, K. S. Colwell, W. A. Goddard, W. M. Skiff, *J. Am. Chem. Soc.* **1992**, *114*, 10024.
- [37] D. E. Coupry, M. A. Addicoat, T. Heine, *J. Chem. Theory Comput.* **2016**, *12*, 5215.
- [38] Y. G. Chung, J. Camp, M. Haranczyk, B. J. Sikora, W. Bury, V. Krungleviciute, T. Yildirim, O. K. Farha, D. S. Sholl, R. Q. Snurr, *Chem. Mater.* **2014**, *26*, 6185.
- [39] P. Dauberoguthorpe, V. Roberts, D. Osguthorpe, J. Wolff, A. H. M. Genest, *Proteins Struct. Funct. Genet.* **1988**, *4*, 31.
- [40] D. Dubbeldam, K. Walton, D. Ellis, R. Snurr, *Angew. Chem. Int. Ed.* **2007**, *46*, 4496.
- [41] N. Allinger, Y. Yuh, J. Lii, *Molecular Mechanics. J. Am. Chem. Soc.* **1989**, *111*, 8551.
- [42] M. Tafipolsky, R. Schmid, *J. Phys. Chem. B* **2009**, *113*, 1341.
- [43] J. S. Grosh, F. Paesani, *J. Am. Chem. Soc.* **2012**, *134*, 4207.
- [44] A. R. Kulkarni, D. S. Sholl, *Langmuir* **2015**, *31*, 8453.
- [45] S. Vandenbrande, M. Waroquier, V. V. Van Speybroeck, T. Verstraelen, *J. Chem. Theory Comput.* **2017**, *13*, 161.
- [46] S. Vandenbrande, T. Verstraelen, J. J. Gutierrez-Sevillano, M. Waroquier, V. Van Speybroeck, *J. Phys. Chem. C* **2017**, *121*, 25309.
- [47] P. G. Yot, L. Vanduyfhuys, E. Alvarez, J. Rodriguez, J. P. Itie, P. Fabry, N. Guillou, T. Devic, I. Beurroies, P. L. Llewellyn, V. Van Speybroeck, C. Serre, G. Maurin, *Chem. Sci.* **2016**, *7*, 446.
- [48] S. Rogge, L. Vanduyfhuys, A. Ghysels, M. Waroquier, T. Verstraelen, G. Maurin, V. Van Speybroeck, *J. Chem. Theory Comput.* **2015**, *11*, 5583.
- [49] S. L. Li, D. G. Truhlar, *J. Chem. Phys.* **2017**, *146*, 064301.
- [50] J. Heinen, N. C. Burtch, K. S. Walton, D. Dubbeldam, *J. Chem. Theory Comput.* **2017**, *13*, 3722.
- [51] T. Verstraelen, L. Vanduyfhuys, S. Vandenbrande, S. M. J. Rogge, *Yaff, yet another force field*, <http://molmod.ugent.be/software/>.
- [52] S. Grimme, *J. Comput. Chem.* **2006**, *27*, 1787.
- [53] S. Grimme, J. Antony, S. Ehrlich, H. Krieg, *J. Chem. Phys.* **2010**, *132*, 154104.
- [54] S. Grimme, S. Ehrlich, L. Goerigk, *J. Comput. Chem.* **2011**, *32*, 1456.
- [55] S. Grimme, *J. Chem. Theory Comput.* **2014**, *10*, 4497.
- [56] J. Maple, M. J. Hwang, T. Stockfisch, U. Dinur, M. Waldman, C. S. Ewig, A. T. Hagler, *J. Comput. Chem.* **1994**, *15*, 162.
- [57] R. Borkman, G. Simons, R. Parr, *J. Chem. Phys.* **1969**, *50*, 58.
- [58] M. J. Frisch, G. W. Trucks, H. B. Schlegel, G. E. Scuseria, M. A. Robb, J. R. Cheeseman, G. Scalmani, V. Barone, B. Mennucci, G. A. Petersson, H. Nakatsuji, M. Caricato, X. Li, H. P. Hratchian, A. F. Izmaylov, J. Bloino, G. Zheng, J. L. Sonnenberg, M. Hada, M. Ehara, K. Toyota, R. Fukuda, J. Hasegawa, M. Ishida, T. Nakajima, Y. Honda, O. Kitao, H. Nakai, T. Vreven, Jr., J. A. Montgomery, J. E. Peralta, F. Ogliaro, M. Bearpark, J. J. Heyd, E. Brothers, K. N. Kudin, V. N. Staroverov, R. Kobayashi, J. Normand, K. Raghavachari, A. Rendell, J. C. Burant, S. S. Iyengar, J. Tomasi, M. Cossi, N. Rega, J. M. Millam, M. Klene, J. E. Knox, J. B. Cross, V. Bakken, C. Adamo, J. Jaramillo, R. Gomperts, R. E. Stratmann, O. Yazyev, A. J. Austin, R. Cammi, C. Pomelli, J. W. Ochterski, R. L. Martin, K. Morokuma, V. G. Zakrzewski, G. A. Voth, P. Salvador, J. J. Dannenberg, S. Dapprich, A. D. Daniels, O. Farkas, J. B. Foresman, J. V. Ortiz, J. Cioslowski, and D. J. Fox, *Gaussian 09 Revision A.02*; Gaussian, Inc.: Wallingford, CT, **2009**.
- [59] G. Kresse, J. Furthmüller, *Comput. Mater. Sci.* **1996**, *6*, 15.
- [60] G. Kresse, J. Furthmüller, *Phys. Rev. B* **1996**, *54*, 11169.
- [61] J. Perdew, K. Burke, M. Ernzerhof, *Phys. Rev. Lett.* **1996**, *77*, 3865.

- [62] A. Becke, *Phys. Rev. A* **1988**, *38*, 3098.
- [63] A. Becke, *J. Chem. Phys.* **1993**, *98*, 5648.
- [64] C. Lee, W. Yang, R. Parr, *Phys. Rev. B* **1988**, *37*, 785.
- [65] S. Zygmunt, R. Mueller, L. Curtiss, L. Iton, *Theochem* **1998**, *430*, 9.
- [66] S. Sousa, P. Fernandes, M. Ramos, *J. Phys. Chem. A* **2007**, *111*, 10439.
- [67] R. Krishnan, J. S. Binkley, R. Seeger, J. A. Pople, *J. Chem. Phys.* **1980**, *72*, 650.
- [68] A. D. McLean, G. S. Chandler, *J. Chem. Phys.* **1980**, *72*, 5639.
- [69] M. J. Frisch, J. A. Pople, J. S. Binkley, *J. Chem. Phys.* **1984**, *80*, 3265.
- [70] W. Zhou, H. Wu, T. Yildirim, J. R. Simpson, A. R. H. Walker, *Phys. Rev. B* **2008**, *78*, 054114.
- [71] N. Lock, Y. Wu, M. Christensen, L. J. Cameron, V. K. Peterson, A. J. Bridgeman, C. J. Kepert, B. B. Iversen, *J. Phys. Chem. C* **2010**, *114*, 16181.
- [72] N. Lock, M. Christensen, Y. Wu, V. K. Peterson, M. K. Thomsen, R. O. Piltz, A. J. Ramirez-Cuesta, G. J. McIntyre, K. Norén, R. Kutteh, C. J. Kepert, G. J. Kearley, B. B. Iversen, *Dalton Trans.* **2013**, *42*, 1996.
- [73] J. C. Tan, A. K. Cheetham, *Chem. Soc. Rev.* **2011**, *40*, 1059.
- [74] S. Yang, J. Sun, A. J. Ramirez-Cuesta, S. K. Callear, W. I. F. David, D. P. Anderson, R. Newby, A. J. Blake, J. E. Parker, C. C. Tang, M. Schröder, *Nat. Chem.* **2012**, *4*, 887.
- [75] F. Niekel, M. Ackermann, P. Guerrier, A. Rothkirch, N. Stock, *Inorg. Chem.* **2013**, *52*, 8699.
- [76] A. U. Ortiz, A. Boutin, F. X. Coudert, *Chem. Commun.* **2014**, *50*, 5867.
- [77] A. M. Walker, B. Civalieri, B. Slater, C. Mellot-Draznieks, F. Corà, C. M. Zicovich-Wilson, G. Román-Pérez, J. M. Soler, J. D. Gale, *Angew. Chem. Int. Ed.* **2010**, *49*, 7501.
- [78] E. Cockayne, *J. Phys. Chem. C* **2017**, *121*, 4312.

Received: 24 November 2017

Revised: 11 January 2018

Accepted: 12 January 2018

Published online on 2 February 2018